169

Seminar on FISSION

Pont d'Oye IV

Castle of Pont d'Oye, Habay-la-Neuve, Belgium
5 – 8 October 1999

Editors

Cyriel Wagemans
University of Gent, Belgium

Olivier Serot
IRMM, Geel, Belgium

Pierre D'hondt
SCK-CEN, Mol, Belgium

World Scientific
Singapore • New Jersey • London • Hong Kong

Published by

World Scientific Publishing Co. Pte. Ltd.

P O Box 128, Farrer Road, Singapore 912805

USA office: Suite 1B, 1060 Main Street, River Edge, NJ 07661

UK office: 57 Shelton Street, Covent Garden, London WC2H 9HE

British Library Cataloguing-in-Publication Data
A catalogue record for this book is available from the British Library.

SEMINAR ON FISSION
Pont d'Oye IV

ISBN 981-02-4241-7

Printed in Singapore by Regal Press (S) Pte. Ltd.

SCK·CEN

Fonds voor Wetenschappelijk Onderzoek - Vlaanderen
Fund for Scientific Research - Flanders (Belgium)

irmn

A THEORETICAL DESCRIPTION OF SPALLATION REACTIONS

J. CUGNON

Université de Liège, Institut de Physique B.5, Sart Tilman
B-4000 LIEGE 1
E-mail: J.Cugnon@ulg.ac.be

Spallation reactions appear as the microscopic processes responsible for the generation of neutrons in so-called spallation sources, which constitute an important part of future ADS systems. The most successful theoretical model for describing these reactions, namely the INC + evaporation model, is briefly reviewed. In particular, the physical content, the performances and the possible improvements, especially concerning fission, are discussed.

1 Introduction

Microscopically, a spallation reaction is the mechanism by which a high energy hadron pulls out of a target nucleus some nucleons and/or light particles, leaving a residual nucleus (sometimes called a spallation product) of mass smaller than but commensurate with the target mass. In the energy range spanning from $\sim$ 100 MeV to $\sim$ 10 GeV, this is by far the most important interaction mechanism. The word *spallation* is also used to denote the macroscopic phenomenon by which a high energy hadron hitting a very thick target, often called a spallation target, expels from it a certain number of particles, basically neutrons in that case. As we explain below, this macroscopic process involves a repetition of microscopic spallation reactions.

Spallation reactions are known for a long time and the basic features have been identified readily by Serber[1]. There is however a renewed interest in these reactions because of the flourishing number of projects of accelerator driven systems (ADS)[2,3,4,5] which are supposed to play an important role for nuclear waste processing in the future. An ADS contains as an important part a spallation source. The optimization of these sources, if realized empirically, would require a tremendous number of measurements of the flux of emitted particles. A generally accepted point of view favours optimization by simulations. As alluded above, this would require the precise knowledge of the elementary hadron-nucleus interactions. The experimental determination of the cross-sections for all exit channels is beyond feasibility. Therefore, also at this level, a general consensus arises on the best solution being the construction of numerical models for generating all possible exit channels, "validated"

by comparison on a few well chosen benchmark measurements. So, in the last years, the theoretical description of spallation reactions has been revisited, aiming at an improvement of the numerical models, on an empiric basis for some features and using new theoretical developments for others. We present below a review of this activity concerning the most successful model, namely the intranuclear cascade (INC) + evaporation model.

It is worth to mention that the understanding and the description of spallation reactions are also of primordial importance for the development of so-called multipurpose spallation sources devoted to material structure analyses[6], for the understanding of spallation induced nucleosynthesis by cosmic rays[7], for production of exotic nuclei [8] and exotic beams [9], and for production and study of hot nuclei [10] and their possible deexcitation by multifragmentation.[11]

This review is organized as follows. Sec. 2 is devoted to a brief description of the phenomena taking place in a thick spallation target. In Sec. 3, we make a survey of experimental data for spallation on thin targets. Sec. 4 is devoted to the description of the INC + evaporation model. Several topics are developed: the predictive power, the possible improvements, the coupling between the two steps of the model (Sec. 5), the input data, especially concerning fission (Sec.6), and the theoretical foundations of the model. Sec.7 is devoted to the accuracy to be achieved when the model is applied to ADS systems. Finally, Sec. 8 contains our conclusion.

2 The basic physics of a spallation source

An impinging high energy hadron will be first slowed down by Coulomb collisions with elections (if charged). Ultimately it will induce a spallation reaction with a target nucleus. A few energetic particles are ejected, which will induce further particle-nucleus interactions, and so on. A sort of (extra-nuclear) cascade happens with particles being less and less energetic. Charged particles are most of time stopped in the target. On the other hand, neutrons can be slowed down and diffuse out of the target. The number of neutrons produced by incident proton has been measured in a few cases. The more relevant parameter, i.e. the number of neutrons per proton and divided by the incident energy[a], is plotted in fig. 1. This determines the optimum regime of incident proton energy, which lies somewhere between 1 and 2 GeV. The spectrum (and the emission pattern) of the escaping neutrons depends upon the detail of the target geometry. Typically the neutron spectrum extends up to a few

[a]This parameter is equal to the energy necessary to generate a neutron. To a large extent it is proportional to the price required to generate a neutron.

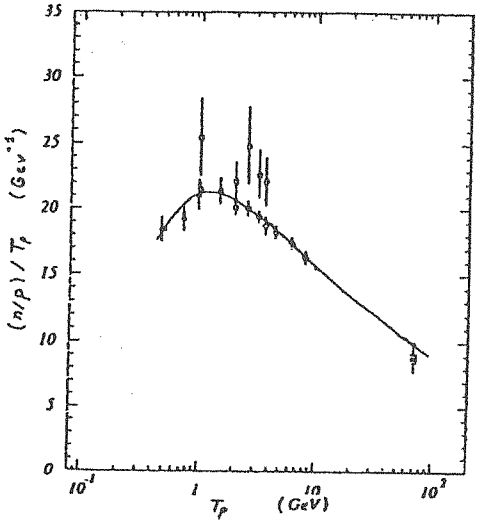

Figure 1. Number of neutrons per proton and per energy as a function of the incident proton energy for a cylindrical lead target of 20 cm diameter and 60 cm length.

MeV, the maximum value depending mainly upon the transverse extension of the spallation target.

Successive particle interactions generate more and more neutrons inside the target up to a certain point. When these neutrons are less energetic, say below 10 MeV, they do not multiply any more and, depending upon the nature of the target, can even be absorbed.

The spallation process changes the nature of some target nuclei, as we illustrate in Sec. 5. Furthermore, these nuclei recoil with an energy which can vary from 0 to a few hundreds of KeV. These phenomena may have severe consequences on the structural properties of the target. Finally, the deexcitation of these nuclei may produce emission of β-rays and sometimes hard γ-rays which may give rise to radiation problems. We do not want to discuss these problems here. See ref.[12] for more information.

3 Experimental survey

We restrict ourselves to nucleon-induced spallation reactions. Direct measurements of particle multiplicity are scarce and rather unprecise. The most

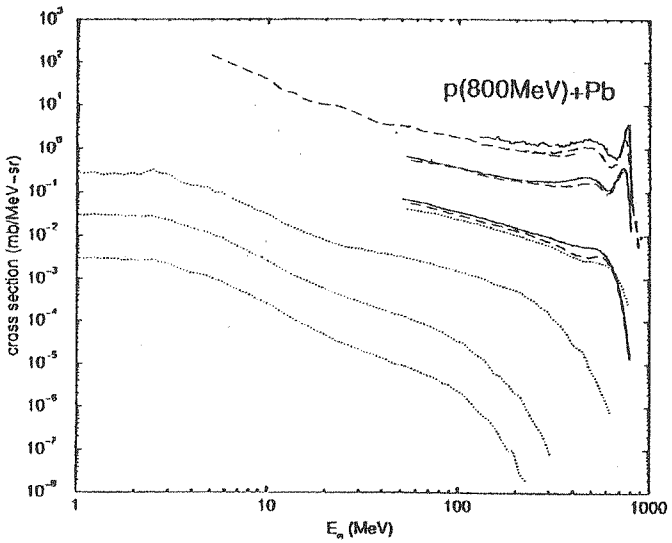

Figure 2. Representation of the available data of neutron double differential cross-section in p(800MeV)+ Pb reaction for 0, 7.5, 30, 60, 120 and 150 degrees from top to bottom. The various curves have been multiplied by 10^{-n} with n=0,1,2... for the sake of presentation.

important result is the overwhelming production of nucleons, and for the latter the dominance of neutrons. Neutron spectra at different angles in p-induced reactions has received some attention, especially recently. For a detailed account, see ref. [13]. We give a typical result in fig. 2. We discuss them a little bit, as they give a hint to the dynamics. On the high neutron energy side, the most striking feature is the presence of a peak (at small angles) at an energy close to the incident energy. This obviously comes from the quasi-elastic process by which the incident proton transfers its energy-momentum to a target neutron and remains more or less at rest in the target. There is another, broader, peak at a neutron energy about $\sim$ 300 MeV below. This peak originates from the quasi-inelastic process, by which the incident proton kicks off a target neutron but remains in the target, being excited to a Δ^+ resonance. On the low energy side ($\leq$ 10 MeV), all spectra are largely independent of the emission angle and look like a Maxwellian distribution. This is a clear signal of an evaporation emission by an excited nucleus. These

observations strongly suggest that the spallation process can be viewed as a succession of nucleon-nucleon collisions. Depending upon the conditions, the number of collisions may be as low as unity or as large as leading to a full thermalization of the nuclear volume. Following to these considerations, it is natural to look for a theoretical description based upon multiple scattering theory. This is explained in the next section.

Before closing this section, let us mention that the residue mass spectrum has also been measured. It of course reflects the sometimes copious emission of particles, but also shows the importance of the fission process, if the target mass is sufficiently heavy (see fig. 6).

4 The INC + evaporation model

4.1 The INC model

This model has been used for nucleon, π, $\bar{p}$,...-nucleus and heavy ion reactions. For a detailed description, see refs.[14,15]. We limit ourselves to a brief outline of the physical picture and of the theoretical basis.

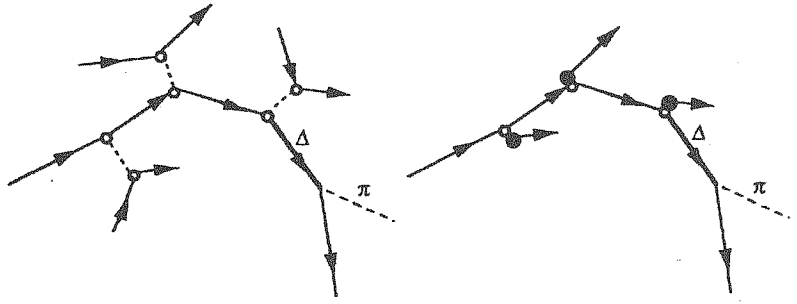

Figure 3. Schematic representation of the INC models of first (left) and second (right) type. In the latter case, nucleons promoted from the continuum are indicated by heavy dots.

In short, the INC model pictures the nucleon-nucleus collision process as a sequence of binary baryon-baryon collisions, occurring as in free space. There are two basic lines of approach (see fig. 3). In the first one (used in the Liège cascade[15]), all particles are propagating freely until a pair of them reaches its minimum distance of approach d_{min}. They are forced to scatter if $d_{min} \leq \sqrt{\sigma_{tot}/\pi}$, in accordance with energy-momentum conservation. The final directions are chosen at random according to the experimental angular distribution. Afterwards, the particles resume straight line motion until the

next collision, and so on. In the second line of approach (like in the BERTINI code[16]), the target is seen as a continuum providing active particles with a mean free path $\lambda = (\rho\sigma_{tot})^{-1}$. After a path, an active particle is supposed to scatter on a nucleon, which is so promoted as a new active particle from the continuum, and so on. In the first type of approach, the time development of the process is studied. This is not the case in the second line of approach where the cascades initiated by active particles are treated independently. Many features are introduced, quite similarly sometimes, in both types of approach: target Fermi motion, Pauli blocking of collisions leading to already occupied states, inelastic collisions, pion production (through Δ excitation basically), (constant) mean field in the target volume and calculations of observables by ensemble averages.

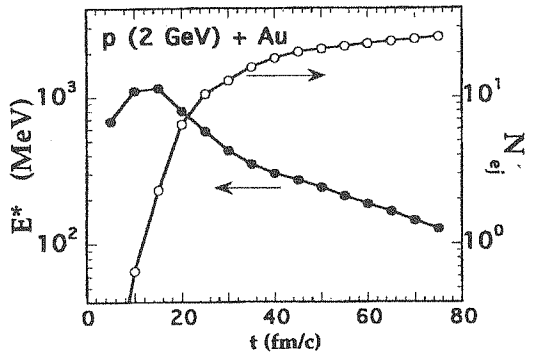

Figure 4. Time evolution of the target excitation (left scale) and of the number of ejectiles (right scale) in b = 2 fm collisions for the indicated system.

Let us discuss shortly the space-time aspects of proton-nucleus interaction in the GeV range, as predicted by the INC model (of the first type). The available incident kinetic energy W_p^0 is progressively shared by the incident particle itself, the pions, the other ejectiles and the target

$$W_p^0 = W_p(t) + W_\pi(t) + K_{ej}(t) + E^*(t), \tag{1}$$

where E^* is the excitation energy of the target (similar conservation law equations can be formulated by for charge, baryon number, momentum and angular momentum). The proton travels through the target in 10 fm/c or so. It has transferred a large fraction of its initial energy to the nucleus, which gets for

a short while a high excitation energy (see fig. 4). The latter is removed to a large extent, and quickly (in $\sim$ 20 fm/c), by emission of fast nucleons and pions. The remaining excitation energy is further released by emission, at a slow pace, of slow nucleons, very much akin to the evaporation process. It is then preferable at this time to stop the INC calculation, record the excitation energy, mass and momentum of the target remnant and crank an evaporation code to describe the further evolution of the system. This procedure is not only more economical (in computation time), but is mandatory. It is well known indeed that evaporation is highly sensitive to correlations in nuclei, whereas INC embodies a pure single-particle picture, as exemplified by the use of a level parameter departing sometimes strongly for the single particle value $a = A/16$.

The necessary conditions for the validity of the INC model are given by

$$\lambda\!\!\!^{-}_B << r_s << \bar{d} \tag{2}$$

where $\lambda\!\!\!^{-}_B$ is the de Broglie wavelength for the relative motion of nucleons, r_s is the range of nuclear forces and $\bar{d}$ is the average distance between neighboring nucleons. This condition is only marginally fulfilled in the nuclear case. Under the same conditions, a nuclear Boltzmann-like transport equation may be derived

$$\frac{\partial f}{\partial t} + \frac{\vec{p}}{m}.\vec{\nabla} f - \left(\vec{\nabla} U\right).\left(\vec{\nabla}_p f\right) + \left(\vec{\nabla}_p U\right).\vec{\nabla} f = \int \frac{d^3p_2}{(2\pi)^3} \int \frac{d^3p_3}{(2\pi)^3} \int \frac{d^3p_4}{(2\pi)^3} \frac{2\pi}{\hbar} |G(12 \to 34)|^2$$
$$\{f_3 f_4 (1-f)(1-f_2) - f f_2 (1-f_3)(1-f_4)\}\, \delta^3(\vec{p})\, \delta(e(p)) \tag{3}$$

where f_i stands for $f(\vec{r}, \vec{p}_i, t)$, the probability of finding a nucleon with momentum $\vec{p}_i$ at time t and place $\vec{r}$. The δ functions stand symbolically for momentum and energy conservation. In addition

$$e(p) = \frac{p^2}{2m} + U(p)$$
$$U(p) = \int \frac{d^3p'}{(2\pi)^3} \langle \vec{p}\vec{p}' | G(\rho(\vec{r})) | \vec{p}\vec{p}' \rangle \tag{4}$$

and G is the (local) Brueckner matrix, solution of

$$G = V + V \frac{Q}{E_{12} - H_{12}} G \tag{5}$$

and describes the in-medium scattering of two nucleons. It can be shown that the INC algorithm is nothing but a Monte-Carlo evaluation of the r.h.s.

of eq.(3) [17], the collision term, the l.h.s. describing just the streaming of the particles. The Boltzmann limit corresponds to $U = 0$, the factors $1 - f$ missing and G replaced by the free T-matrix. The nuclear Boltzmann equation provides a systematic way of introducing in-medium corrections. Let us finally mention that the INC model does more than solving the Boltzmann equation as it also propagates correlations to any order and do not rest on the hypothesis of molecular chaos [18].

4.2 The evaporation model

There exists many versions of this model, differing mainly by input data. Most of the time, the evaporation of light particles is described by the Weißkopf-Ewing model [19]. The partial width for decay $B \rightarrow A + a$, corresponding to the energy conservation equation $E_B^* = E_A^* + S_a + \epsilon_a$ where S_a and ϵ_a are respectively the separation energy and the kinetic energy of particle a, is given by

$$d\Gamma_a = \sigma(aA \rightarrow B) \frac{2m_a}{(2\pi)^3 \hbar^2} \frac{\rho(E_A^*)}{\rho(E_B^*)} \epsilon_a d\epsilon_a \tag{6}$$

In this equation, $\sigma(aA \rightarrow B)$ is the capture cross-section of particles a by nuclei A and ρ is the density of states.

The fission channel partial width (at low excitation energy) is usually evaluated by the transition state method

$$d\Gamma_f = \frac{1}{2\pi} \frac{\rho\left(\tilde{E}_B^*\right)}{\rho(E_B^*)} d\epsilon_a^? \tag{7}$$

where $\tilde{E}_B^*$ represents the excitation energy at the fission barrier.

In the evaporation model, the emission in a particular channel is determined stochastically according to the relative values of the various partial widths. This procedure is repeated until the excitation energy has fallen down below the lowest emission threshold.

The basic input data in the evaporation-fission models are thus capture cross-sections, often taken as geometric cross-sections, fission barriers and density of states. The latter is the most crucial quantity, as the dependence of partial widths upon this quantity is rather strong (see below). Furthermore, the behaviour of the density of states at high excitation energy is badly known.

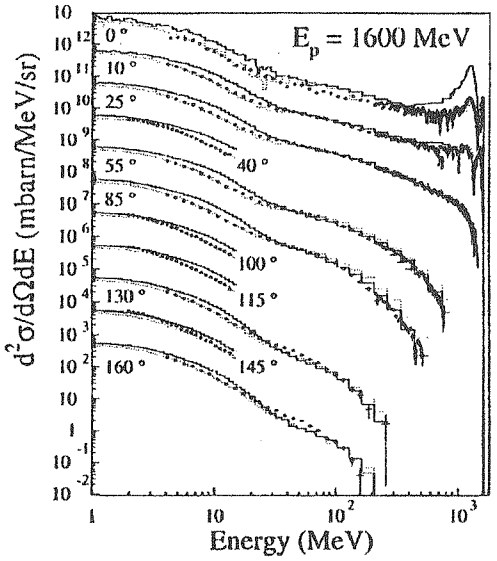

Figure 5. Double differential cross-section for neutron production in p(1600MeV)+Pb collisions. Data from ref.[26] (dots) are compared with the Bertini (full histograms) and Liège (dotted histograms) INC + evaporation models. Adapted from ref.[26].

4.3 The INC + evaporation model. The stopping time

As explained above, in the INC models of the first type, there is a time at which the rate of energy release from the target drops sizeably. This can be taken as the stopping time, the time at which the INC gives way to evaporation. It has to be noted, however, that this time is at best determined with an accuracy of 5 fm/c or so. In the INC models of second type, the cascade is stopped not at a definite time, for there is no time structure, but by ending the collision sequence when the kinetic energy of particles is below a cut-off value, left as a free parameter. The two procedures can hardly be compared [15].

5 Results

In fig.5 , we give a typical result concerning the neutron double differential cross-sections. The agreement is rather good, although the cross-section at high neutron energy and very forward angles is underestimated. Fig.6 displays typical results for the residue mass distribution. Once again, the agreement is rather good. Discrepancies at large residue mass is nevertheless to be mentioned. Possible improvements are studied actively [15].

Let us discuss however the influence of the stopping time, the only real parameter in the INC models of the first type. If this time is varied, increased e.g., there will be a little bit less of neutrons emitted in the cascade stage with energy around 10 MeV, but this will be compensated by a little extra quantity of neutrons emitted in the beginning of the evaporation stage, i.e. in the same energy range. Neutron spectra are thus largely independent of the stopping time. For the residue mass spectrum, the sensitivity is higher. Indeed if, in some event, the INC generates a primary residue of mass A_{PR} at excitation energy E^*, the final residue will have mass A_R given by

$$A_R = A_{PR} - E^*/\langle \epsilon_p + S_p \rangle \tag{8}$$

where the average is taken on all emitted particles. Grossly speaking, the mass A_{PR} is largely independent of the stopping time [15]. But the excitation energy E^* does depend more appreciably in this time (see fig.4). Alternatively, it can be said that the residue mass spectrum is sensitive to the excitation energy at the beginning of the evaporation stage.

6 Fission aspects

Spallation reactions on heavy targets present a unique feature: the fission of a primary residue with high excitation energy E^* and low angular momentum. In a p+Pb reaction at 1 GeV, E^* is expected to be $\sim$ 150 MeV, on the average, but may reach 600 MeV. Similar excitation energies are reached in heavy ion reactions, but they are accompanied with a large angular momentum.

In such conditions, ordinary evaporation/fission statistical models are doubtful. Indeed, from Eqs. (6-7), one obtains

$$\frac{\Gamma_n}{\Gamma_f} = \frac{4m_n}{\pi\hbar^2} \frac{\int_0^{E^*-S_n} \epsilon\sigma(aA \to B)\rho\left(E^* - S_n - \epsilon\right) d\epsilon}{\int_0^{E^*-B_f} \rho\left(E^* - B_f - \epsilon\right) d\epsilon} \tag{9}$$

where B_f is the fission barrier height. In the numerator the density of states refers to the compound system. In the denominator, it refers to the system

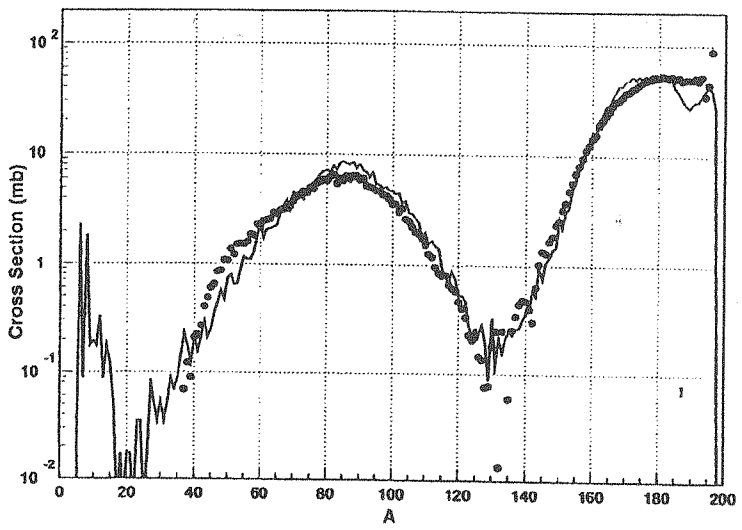

Figure 6. Cross-section for production of residue of mass number A in Au(800MeV/A)+p collisions. Data from ref.[24] (dots) are compared with the Liège INC + evaporation model.

at the barrier. Taking for simplification the two densities of states as $\rho \sim exp\left(2\sqrt{aE^*}\right)$, with different level parameters, one obtains for large E^*:

$$\frac{\Gamma_n}{\Gamma_f} \propto \sqrt{\frac{a}{a_f}}\, e^{2\left(\sqrt{a}-\sqrt{a_f}\right)\sqrt{E^*}} \tag{10}$$

This ratio does depend sensitively upon the level parameters for increasing E^*. If $a_f > a$, as it is customarily assumed, $\Gamma_n/\Gamma_f \to 0$ at large E^*, which is doubtful, since the time necessary to evaporate a neutron is then much smaller than typical fission times [20]. In popular models [5], formula (10) is empirically modified for large E^*.

To account for time scales which are absent in a purely probabilistic model, it is usually advocated to turn to Kramers formulation of fission width [21], which accounts for friction forces along the fission path. These forces can considerably reduce the fission width. For instance, for large friction param-

eter γ, one has

$$\Gamma_f = \frac{\hbar\omega_0\omega_b}{2\pi\gamma}\, e^{-\frac{B_f}{T}} \qquad (11)$$

where ω_0 and ω_b are the curvatures of the inner well and of the barrier along the fission parameter, respectively, and where T is the temperature $\left(T \simeq \sqrt{E^*/a}\right)$.

However, a complete time-dependent picture seems to be unavoidable. Indeed, it has been shown, in the heavy ion case, that, at high excitation energy, the system cools down significantly by neutron emission, along the path to fission [22]. Kramers formula are no longer valid. It has been shown [23] that strong deviations from Kramers formula occur for low neutron multiplicity. Taking account of this feature considerably lengthens the calculations as this implies solving Fokker-Planck equation in two dimensions. This point is also discussed in ref.[24].

7 Required accuracy

This point can be discussed in the following general framework. Reactor designers use numerical codes to calculate the neutron flux, the multiplication factor k_{eff} and the power distribution in an ADS. They need as input the flux of neutrons $\phi\,(r, z, \Omega, E_n)$ getting out of the spallation target at coordinates (r, z) in the direction Ω with energy E_n. This can be provided by transport codes describing the propagation of particles inside a spallation target. These codes need as input the n-tuple differential cross-section $d^n\sigma/d^3p_1...d^3p_n$ for producing any number n of particles in a spallation reaction. The latter can be simulated in a INC + evaporation code.

The accuracy required for the prediction of reactor parameters is of the order of 1 % (at least for k_{eff}). According to the experts, this requires an accuracy of about 10 % in the multiplicity of the neutrons issued from the spallation source (the integrated value of ϕ above) and about 30 % for the distribution of ϕ itself [25]. Which accuracy is required for the predictions of the INC + evaporation model to guarantee such an accuracy for the predictions of transport codes is not known. However, it seems reasonable to require the same level of accuracy. Around 1 GeV, this goal is not far from being attained (see fig.4).

8 Conclusion

We have reviewed here the main aspects of the INC + evaporation model, emphasizing the empirical and theoretical foundations of the model. We discussed the question of the proper coupling between the two stages of the model. We also give an illustration of the success of the model and of its possible improvements, especially concerning fission. In addition, we discussed shortly the necessary accuracy for this model to be useful for the conception of ADS systems.

References

1. R. Serber, *Phys. Rev.* **72**, 1114 (1947).
2. C.D. Bowman *et al*, *Nucl. Instrum. Methods* **A320**, 336 (1992).
3. C. Rubbia *et al*, in *Conceptual Design of a Fast Neutron Operated High Power Energy Amplifier*, Preprint CERN/AT/95-44 (ET) 1995.
4. S. Matsura, *Nucl. Phys.* A **654**, 417c (1999).
5. H. Aït Abderrahim, Ch. De Raedt and E. Malambu, The MYRRHA Project, these proceedings.
6. P. M. Garvey, Proc. of the Meeting on Target for Neutron Beam Spallation Sources, Julich, Jul-Conf-34, ISSN0344-5789, 1980.
7. R. Michel *et al*, *Nucl. Instrum. Methods* **B103**, 183 (1995).
8. A.C. Müller, *Nucl. Phys.* A **654**, 215c (1999).
9. I. Tanihata, *Nucl. Phys.* A **654**, 235c (1999).
10. B. Lott *et al*, *Nucl. Phys.* A **654**, 803c (1999).
11. D. Durand, *Nucl. Phys.* A **654**, 273c (1999).
12. O. Bersillon *et al*, Contribution to the 2nd International Conference on Accelerator-Driven Transmutation Technologies and Applications, Kalmar, Sweden, 1996.
13. J. Cugnon, Ecole Joliot-Curie, 1996.
14. J. Cugnon, *Nucl. Phys.* A **462**, 751 (1987).
15. J. Cugnon, C. Volant and S. Vuillier, *Nucl. Phys.* A **620**, 475 (1997).
16. H.W. Bertini *et al*, *Phys. Rev.* **131**, 1801 (1963).
17. V.E. Bunakov and G.V. Matvejev, *Z. Phys.* A **322**, 511 (1985).
18. J. Cugnon, *Nucl. Phys.* A **389**, 191c (1982).
19. V.F. Weißkopf and D.H. Ewing, *Phys. Rev.* **57**, 472,935 (1940).
20. T. Ericson, Advances in Physics, **9**, 425 (1960).
21. H.A. Kramers, *Physica* VIII N.4, 284 (1940).
22. E. Holub *et al*, *Phys. Rev.* C **28**, 252 (1983).
23. H. Delagrange *et al*, *Z. Phys.* A **323**, 437 (1986).

24. J. Benlliure, these proceedings.
25. R. Salvatores, private communication.
26. X. Ledoux *et al*, *Phys. Rev. Lett.* **82**, 4412 (1999).